Revue des Energies Renouvelables Vol. 16 N°3 (2013) 585 – 597

Thermal performances of a bioclimatic building in hot and dry tropical climate

O. Coulibaly [1*], A. Ouedraogo [2†], J. Koulidiati [1] and P. Abadie [3‡]

[1] Laboratoire de Physique et Chimie de l'Environnement, LPCE
[2] Laboratoire des Energies Thermiques et Renouvelables, LETRE
Université de Ouagadougou, 03
B.P. 7021 Ouagadougou 03, Burkina Faso
[3] Conseil Juridique, Expert-comptable, 01 B.P. 964, Ouagadougou 01, Burkina Faso

(Reçu le 20 Juin 2012 – accepté le 30 Septembre 2013)

Résumé - *Le présent travail concerne l'étude du confort bioclimatique d'un bâtiment à sept étages construit avec des matériaux locaux. Dans un premier temps, on utilise un code informatique pour analyser l'impact de l'inertie thermique des matériaux de construction sur l'optimisation de l'enveloppe du bâtiment. Deuxièmement, les températures intérieure et extérieure sont déterminées en utilisant le code TRNSYS. Un système de trappe est conçu de manière à évacuer durant la nuit l'énergie emmagasinée pendant la journée. Les différences entre les charges thermiques de climatisation du bâtiment en double et simple murs sont évaluées. De même, les coefficients des pertes thermiques linéaires et des ponts thermiques sont calculés en utilisant respectivement le logiciel 'Heat' et la méthode des degrés-jour. Les résultats montrent une différence de 6 à 7 ^{o}C entre les maximas des températures des surfaces intérieures et extérieures. On obtient en outre un gain énergétique estimé à 5.8 % dans les salles de bureaux et 12.1 % dans les chambres à coucher et respectivement pour les double et simple murs. Les pertes thermiques au niveau des ponts pour les doubles murs représentent 16.46 % de l'ensemble des pertes du bâtiment et 20.77 % pour le mur simple de 20 cm d'épaisseur. Les investigations du confort thermique se poursuivent avec l'examen de l'addition d'un gardien toiture.*

Abstract - *This paper is concerned with the thermal comfort of a double-walls seven stories bioclimatic building built with local construction materials. First of all, we use a numerical code to investigate the construction materials thermal inertia effects on the optimization of the building envelop. Second, the outer and inner surface temperatures are determined utilizing the TRNSYS code. A system of trap is then design to evacuate during nighttimes, the stored daily heat. The conditioned air thermal load differences between the double and simple walls are also investigated. Similarly, the linear thermal loss coefficients and the thermal bridge losses are computed utilizing respectively the 'Heat' software and the Degree Day method. The results show a difference of 6 to 7 ^{o}C between the outer and the inner maxima surface temperatures. The computation of the conditioned air thermal load indicates a net energy gain of the order of 5.8 % in the office spaces and 12.1% in the bedrooms, respectively for the double and simple walls. The double-walls thermal bridge losses amount to 16.46 % of the total building losses and 20.77 % for the 20 cm thick simple wall. The building envelop optimisation process continues with the study of the effects of the addition of a garden roof on the thermal comfort.*

[*] ousmane.coulibaly@univ-ouaga.bf; jean.koulidiati@univ-ouaga.bf
[†] abdoulay@univ-ouaga.bf
[‡] pierre@abadie.bf

Keywords: Bioclimatic - Tropical climate - Building envelop - Construction materials - Thermal inertia - Thermal performances - Thermal comfort - Thermal bridge - Heat software - TRNSYS software.

1. INTRODUCTION

The bioclimatic architecture makes an intelligent dosage of the existing potential in order to reach an inner climate which respects individual comfort, while adapting to local climatic variability. If properly achieved, it sets a joyful relationship between the occupants and the environment. Therefore, it is difficult to define a unique type of bioclimatic architecture because of the diversity of climate. In the tropical region, the comfort zone might be reached with air conditioner or by bioclimatic design (IEPF, 2008). The public building energy consumption in Burkina Faso, especially for conditioned air, amounts to 30000 MWh/year, an expenditure of 3.4 Billions of CFA Francs/year (DGE, 2003) or 52 Millions of Euros, approximately. These financial loads weight heavily on the development potential of most sub-Saharan countries. It is therefore essential to promotion bioclimatic building as a mean of reaching the thermal comfort and controlling in the same time the huge energy consumption. The investigated building, called 'Newango', is localized at Ouagadougou, the capital city of Burkina Faso.

2. THERMAL INERTIA

The thermal inertia of a building is a direct function of its thermal capacity, hence, is the product of the mass of all occupants by the specific heat. The thermal capacity (the capacity of a building to absorb energy) behaves like a heat absorber, that is, it resists to any type of brutal energy fluctuation. O. Sidler, 2003, has indicated that the thermal inertia is one of the necessary but not sufficient conditions to reach thermal comfort. The literature (Claessens *et al.*, 2003, CSTB, 2000) suggests a building typology, function of the coefficient α:

$$\alpha = \frac{\text{mass of the building}}{\text{surface of the floor}} \tag{1}$$

- $\alpha < 75\ \text{kg/m}^2$ Light building
- $75 < \alpha < 300\ \text{kg/m}^2$ Average building
- $300\ \text{kg/m}^2 < \alpha$ Heavy building

Another way of characterizing the thermal inertia is through the so called time constant, which is computed from the following relation (Roux, 1984):

$$\tau = R \times C_p \tag{2}$$

where R is the wall thermal resistance (m^2K/W) and C_p its surface thermal capacity (Wh/m^2K). We can determine the phase lag in radian utilizing relation (3):

$$t_r = \sqrt{\pi \times C_r} \tag{3}$$

A numerical code has been designed to compute the daily time lag when we vary the thickness and the nature of the wall construction material layers. A careful analysis of the results of the twelve months hourly daily temperatures of the city of Ouagadougou, leads us to choose case 3 with the following layer dimensions:

Table 1: Wall construction materials and time lag

Wall configuration	Materials layers and thickness (m)							Time lag (h)
	Cement finish	Cement bricks	Poly styrene	Air	Poly urethane	Cement bricks	Cement finish	
Case 1: F.B.S.A.B.F[a]	0.025	0.10	0.02	0.03	0.00	0.10	0.015	13.05
Case 2: F.B.U.B.F[b]	0.025	0.10	0.00	0.00	0.02	0.10	0.015	14.13
Case 3: F.B.A.B.F[c]	0.025	0.20	0.00	0.05	0.00	0.10	0.015	12.28
Case 4: F.B.F[d]	0.025	0.40	0.00	0.00	0.00	0.00	0.015	13.48

a. F-B-S-A-B-F: Finish – Bricks - Polystyrene – Air – Bricks – Finish
b. F-B-U-B-F: Finish – Bricks - Polyurethane – Bricks – Finish
c. F-B-A-B-F: Finish – Bricks – Air – Bricks – Finish
d. F-B-F: Finish – Bricks - Finish

Bricks: 20 cm, Air: 5 cm, Bricks: 10 cm. The thicknesses of the inner an outer finish are the same for all configurations. This selection takes also in account its workability during construction. For the validation, we compute the inner and outer surface temperatures when varying the daily time lag and the heat absorption utilizing the TRNSYS code.

3. INVESTIGATION UTILIZING TRNSYS

The layout of the seven stories building is described with the help of the multizone (Type 56) TRNSYS code (Klein *et al.*, 2006). The photo of the building is shown in the appendix. The hourly temperature data collected by the national meteorological office have been utilized. The air conditioner starts running when the inner temperature exceed 26 °C with a relative humidity of 50 %. Many published results have inspired this undertaken.

They are: the TRNSYS thermal inertia model has been studied by Catalina *et al.*, 2008, and the energy consumption by Al-Ajmi *et al.*, 2008; Annabi *et al.*, 2006; Coulibaly *et al.*, 2010. The fan and the infiltration air are set equal to one volume per hour. Since the objective is to study the behaviour of the double-walls, the interior energy load has not been computed. In summary, the assembly shown in figure 1, works like this:

- Input data.

- Compute the short and long wave's radiation functions, the equivalent temperature of the sky, the psychometric parameters and the ground temperature.

- Compute the building thermal load utilizing the multizone building model (Type 56).

- Finally, output the results.

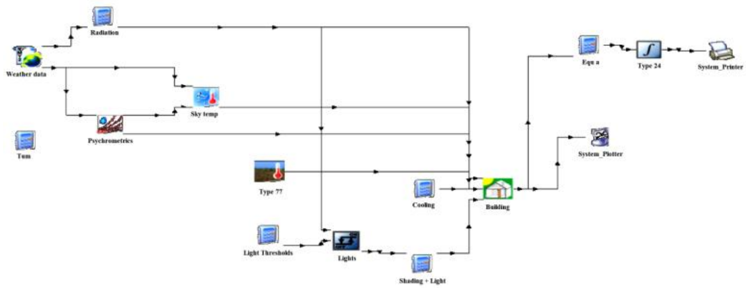

Fig. 1: Modules assembly for building description in TRNSYS

3.1 Surface temperatures

Analysis of Figure 2 indicates that the double-walls is very inertial since it shows little temperature variation all day long (24 h) and only a difference of 6 to 7 °C is observed between the inner and outer maximal temperatures.

During investigations of a bioclimatic hospital localized few miles from Ouagadougou and constructed with compressed mud bricks, the temperature has been lowered down to the interval of 5 – 6 °C below the outer temperature (IEPF, 2008). To ensure the comfort, a trap system is designed in order to evacuate during nigh times, the stored daily heat. The temperatures of the remaining hot months are shown in Appendix B.

The double-walls with the trap system is found to be useful during day and night times. The unit behaves like a simple wall of 10 cm thickness, allowing the evacuation of stored daily heat. After closing the trap system in the morning, the inner temperature which is low remains quite constant all day long because of the inertial strength of the double-walls. However, this result needs to be checked experimentally.

The trap system is designed along the external wall surface, comprising a lower trap at ground level and concrete designed upper trap, such that the lower air duck is wider, inducing a thermo-siphon effect.

3.2 Conditioned air head load: influence of the wall

Figure 3 shows the conditioned air monthly loads. Two picks are clearly visible. They correspond to two hot seasons, the longest which goes from March to June and the shortest especially during the month of October.

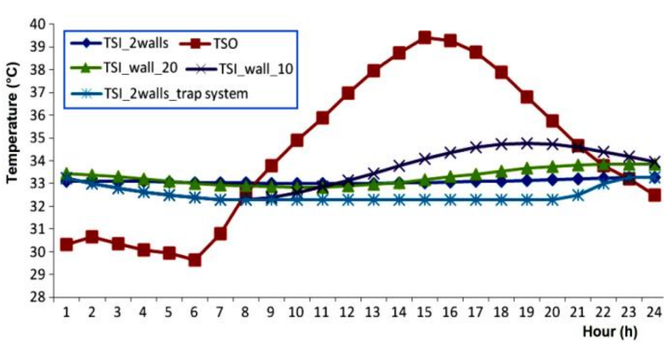

Fig. 2: Time lag and heat absorption during April

The heat load is lower respectively during November to February and during the raining season, June to September. This result is compatible with the local climate.

Figure 4 presents the office space and bedrooms monthly conditioned air thermal loads.

Figures 5 and 6 reveal that the double walls consume less energy than the simple wall.

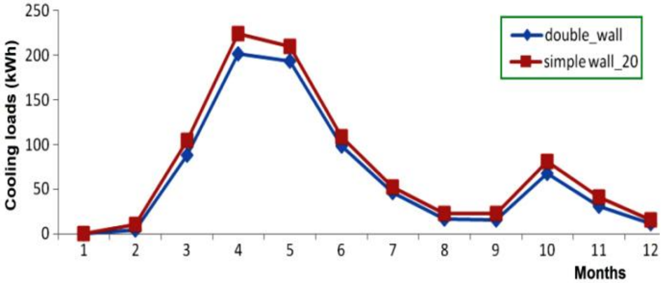

Fig. 3: Monthly conditioned air heat load

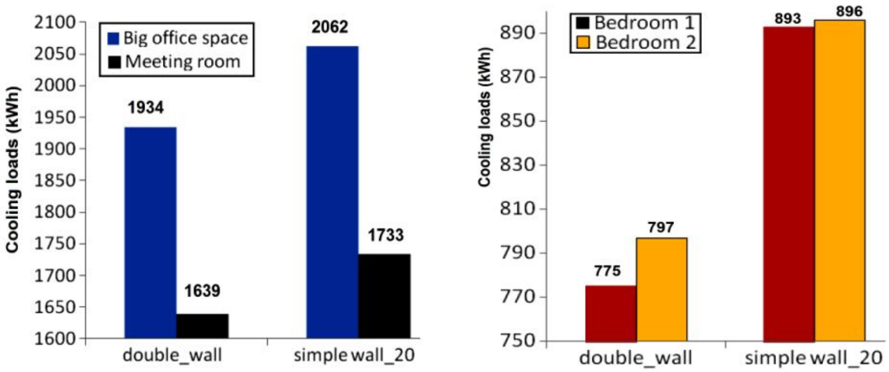

Fig. 4: Double and simple walls conditioned air heat loads

Besides the nature of the wall, the type of building occupancy has been accounted for. In the office space, occupied during day times, the heat load differences between double and simple walls amount to 5.8 %.

In the bedrooms, these energy economies increase up to 12.1 %, which confirms the usefulness of the double-walls during day and night times, **Table 2**.

3.3 Influence of window glazing on conditioned air heat load

These investigations, carried out for the first time set the variations of the conditioned air heat load as a function of different types of window glazing in hot and dry tropical climate. As expected, the load decreases from simple to triple glazing but the percentage in different rooms is quite small (about 9 %). For fact, we see that the energy saving which might be realized with the choice of a given type of glazing, **Table 4**, is not sufficient enough to justify a return of investment. Hence, when an important solar protection is needed, the double glazing is not economical. However, for the comfort, it might be necessary to utilize the double glazing; since in order to reach the comfort zone, we must optimize all surfaces of heat exchange.

Table 2: Conditioned air heat load differences between double and simple walls

Occupancy	Double-walls (kWh)	Simple wall_ 20 cm (kWh)	Differences (kWh)	Differences (%)
Big office space	1933.78	2062.03	128.25	06.22
Meeting room	1639.47	1733.25	93.78	05.41
Bedroom 1	775.30	893.18	117.88	13.20
Bedroom 2	797.09	896.24	99.15	11.06

Table 3: Conditioned air heat load due to window glazing

Zones room				Bedroom1	Bedroom2	Big of. Space	Meeting
Number windows / room				1	2	1	3
Windows characteristics		$U (W/m^2.K)$	G	Heat load (kWh)			
S. glazing	S. glazing	5.7	0.855	722.80	731.07	1797.08	1639.76
D. glazing	D. glazing	1.4	0.589	693.68	682.03	1744.62	1473.47
D. glazing	SHA2AR1	1.3	0.397	693.20	681.36	1743.69	1470.68
S. glazing	Single	5.8	0.855	711.37	707.28	1778.89	1573.75
T. glazing	INS3-KR1	0.7	0.407	691.66	679.27	1740.78	1461.81
T. glazing	INS3-XE2	0.4	0.408	690.94	678.22	1739.50	1457.99

Table 4: Differences in conditioned air heat load (kWh)

Zones		Bedroom1	Bedroom2	Big of. Space	Meeting
Number windows / room		1	2	1	3
D. glazing	D. glazing	29.12	49.03	52.45	166.29
D. glazing	(SHA2AR1)	29.60	49.74	53.39	169.09
S. glazing	(Single)	11.43	23.79	18.19	66.01
T. glazing	(INS3-KR1)	31.14	51.80	56.29	177.95
T. glazing	(INS3-XE2)	31.86	52.84	57.57	181.77

3. INVESTIGATION OF THERMAL BRIDGE UTILIZING THE HEAT CODE

3.1 The HEAT software

The HEAT software permits the simulation of thermal bridges and the computation of the equivalent thermal conductivity of a composite wall in steady state or time dependant variables. HEAT2 and HEAT3 software deal respectively with the simulations in two and three dimensions. The software has been developed at Lund University based on finite volume analysis with variable grid space and capable of solving many configurations problems (Blomberg, 2000).

The governing heat conduction equation in cartesian coordinates in two dimensions is model as follows:

$$\frac{\partial}{\partial x}\left(\lambda_x \times \frac{\partial T}{\partial x}\right) + \frac{\partial}{\partial y}\left(\lambda_y \times \frac{\partial T}{\partial y}\right) + I(x,y,t) = C \times \frac{\partial T}{\partial t} \tag{4}$$

Where I (W/m^3), represents the internal heat sources. The conductivity along the x and y axes is assumed equal; $C = \rho C_p$ ($J/(m^3K)$), is the volumetric thermal capacity.

The source terms are often inexistent and in steady state conditions, the second member is nil.

Two types of boundary conditions are often used; the first condition is linked to the surface resistance and the second to time dependant function $f(t)$.

$$T_{bs}(t) - T\big|_{surf} = R \times (-\lambda)\frac{\partial T}{\partial n}\bigg|_{surf} \tag{5}$$

$$(-\lambda)\frac{\partial T}{\partial n}\bigg|_{bs} = f(t) \tag{6}$$

If the contact is perfect between two materials, we have:

$$(-\lambda_1)\frac{\partial T}{\partial n}\bigg|_1 = (-\lambda_2)\frac{\partial T}{\partial n}\bigg|_2 \tag{7}$$

On the other hand, if the contact is not perfect, then:

$$(-\lambda_1)\frac{\partial T}{\partial n}\bigg|_1 = \frac{T|_2 - T|_1}{R_{ins}} = (-\lambda_2)\frac{\partial T}{\partial n}\bigg|_2 \tag{8}$$

3.2 Determination of the thermal bridge's k coefficient

We are concerned here with losses due to the discontinuities of the wall, directly linked to the geometry and/or to the construction materials. The fact is that, these surfaces show less resistance to heat transfer than other parts of the wall because at these particular locations, the wall is made of much higher thermal conductivity construction materials or has different geometries.

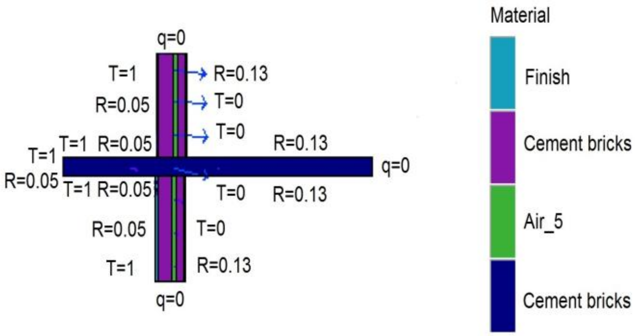

Fig. 5: Double-walls thermal bridge boundary conditions

We compute these anomalies by defining the linear thermal loss coefficient k. The determination of this coefficient with HEAT comes down to computing the corresponding thermal heat flux according to two configurations: with and without the thermal bridge. Now, the thermal bridge heat flux is taken to be the difference between the two computed fluxes.

<u>Nomenclature of figures 5 to 8</u>: T - Temperature, R - Surface resistance, q - Heat flux.

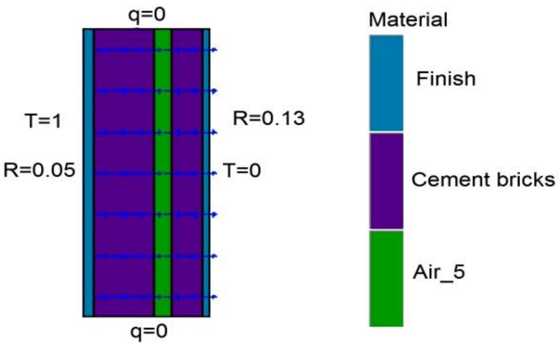

Fig. 6: Boundary conditions of double-walls without thermal bridge

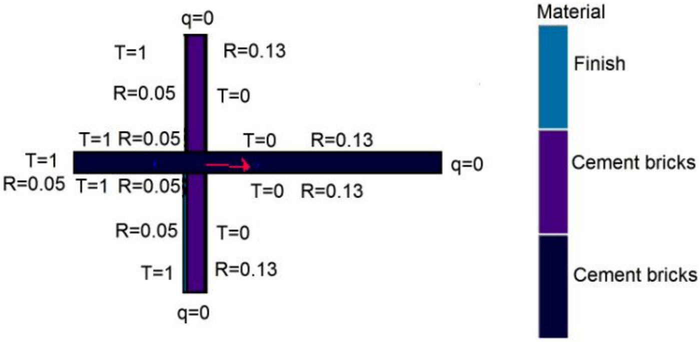

Fig. 7: 20 cm thick simple wall thermal bridge boundary conditions

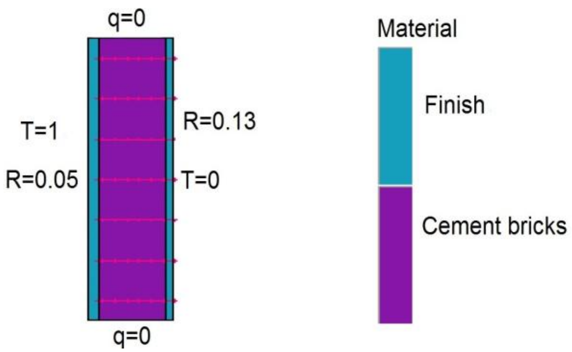

Fig. 8: Boundary conditions for the 20 cm thick simple wall without thermal bridge

Table 5: Heat fluxes values obtained with HEAT and the k coefficient

Characteristics	Total flux (W/m.K)	k coefficient (flux difference) (W/m.K)
Double-walls thermal bridge	6.73	0.58
Double-walls	6.15	
20 cm wall thermal bridge	10.80	0.89
20 cm wall	9.91	

3.3 Computation of the thermal bridge losses utilizing the Degree Day method

The Degree Day represents the positive variation between the outer and the inner temperatures. The Cooling Degree Day (CDD) may be computed with the following relation (Kreith *et al.*, 1978; Stathopoulou, 2006):

$$DJR = (1/24) \times \sum [T_{hr} - T_{bre}]^{+} \tag{9}$$

In this relation,

T_{hr} is the daily hourly temperature for each month and year concerned;

T_{bre} is the basic (base line) cooling temperature;

The + sign is an indication that only positive values are taken in account. That is, if $T_{hr} < T_{bre}$, then $CDD = 0$.

$[T_{hr} - T_{bre}]^{+}$ represents the Cooling Degree Hour (CDH).

Because of the cooling, the thermal gain power for the thermal zone is given by:

$$P_i = \sum_j K_j \times S_j \times (T_e - T_i) + \sum_m K_m \times l_m \times (T_e - T_i) + C_v \times N_i \times V_i \times (T_e - T_i) \tag{10}$$

The first term of the second member represents the transfer gain; the second is concerned with the thermal bridge gain while the last term combines the infiltration and the recycling air contributions.

One infers from the above relation, the expression of the energy necessary for the cooling due to the outer and inner temperature differences (Kreith, 1978).

$$E_{re} = \int_n 86.4 \times G \times V \times [T_{e,n} - T_{bre}]^{+} \times dt \tag{11}$$

E_{re}, expressed in (kJ), G, (W/m^3°C) is the building global transfer coefficient and represents the power losses par unit volume for the outer and the inner temperature differences of 1 °C.

It represents particularly the thermal characteristics of the building envelop, in steady state conditions. V is the building volume and n the number of days. For the thermal bridge, the equivalent expression is written as follows:

$$E_{re} = \int_n 86.4 \times k \times l \times [T_{e,n} - T_{bre}]^{+} \times dt \tag{11}$$

Equation (11) may be written in a summation form:

$$E_{re} = 86.4 \times k \times l \times DJR \tag{12}$$

Table 6: DD and monthly thermal bridge losses for double and simple walls

Months	CDD (°C)	Double-walls		Simple wall _ 20 cm	
		Power (W)	Energy (kWh)	Power (W)	Energy (kWh
January	17.83	96.82	2.32	148.39	3.56
February	60.19	326.85	7.84	500.95	12.02
March	168.47	914.86	21.96	1402.14	33.65
April	225.96	1227.05	29.45	1880.61	45.16
May	206.00	1118.66	26.85	1714.49	41.15
June	123.13	668.64	16.05	1024.78	24.59
July	65.62	356.34	8.55	546.14	13.11
August	216.07	216.07	5.19	331.16	7.95
September	58.69	318.71	7.65	488.46	11.72
October	116.81	634.32	15.22	972.18	23.33
November	68.81	373.66	8.97	572.69	13.74
December	20.93	113.66	2.73	174.20	4.18
Total	**1172.23**	**6365.65**	**152.78**	**975619**	**234.15**

The precedent results show that the thermal bridge losses reach 16.46 % of the building total losses for the double-walls and 20.77 % for the 20 cm thick simple wall.

Table 7: Thermal bridge losses in bedroom 1

Characteristics thermal	**Envelop losses** (kWh)	**Thermal bridge losses** (kWh)	**Total losses** (kWh)	**% for the bridge (%)**
Double walls	775.30	152.78	928.07	16.46
Simple walls 20 cm	893.18	234.15	1127.33	20.77

Acknowledgement- We thank Mr P. Abadie the owner of 'Newango' building for authorizing these investigations and for fruitful discussions. Thank also to the engineers and the architects involved in the project.

4. CONCLUSION

The actual study is part of a much larger research effort to gather enough and reliable scientific data for the design of the country's energy regulation code. As indicated in the introduction, the sahelian countries pay huge amount of money each year for imported oil expenditure.

A large part of this oil is utilized for running air conditioners. These investigation seek therefore to locate on the building envelop all possible areas where energy might be saved. Hence, we study first of all the thermal inertia of the building which is directly linked to the wall construction materials.

Then we choose samples of local composite materials which we validate by computing the inner and outer surface temperatures utilizing the TRNSYS code and find the double-walls to be quite inertial. Next, a trap system is designed which keeps the low temperature of the morning constant all day long. However, this finding needs to be checked experimentally.

Third, we investigated for the first time the influence of window glazing on the thermal load in hot and dry climate. The double glazing is found to be uneconomical but necessary for comfort purpose. Other area of heat losses are the thermal bridges which occur when higher thermal conductivity construction materials exist in the wall.

Finally, the investigation process continues with the addition of a garden roof and the evaluation of its functionality and performances.

REFERENCES

[1] F.F. Al-Ajmi and V.I. Hambi, '*Simulation of Energy Consumption for Kuwaiti Domestic Buildings*', Energy and Buildings, Vol. 40, pp. 1101 - 1109, 2008.

[2] M. Annabi, A. Mokhtari and T.A. Hafrad, '*Estimation des Performances Energétiques dans le Contexte Maghrébin*', Revue des Energies Renouvelables, Vol. 9, N°2, pp. 99 - 106, 2006.

[3] T. Blomberg, '*Heat2, Version 5: A PC-Program for Heat Transfer in Two Dimensions*', Manual with Brief Theory and Examples, Lund-Gothenburg Group for Computational Building Physics, 183 p., 2000.

[4] J. Claessens, Y. Coulibaly, T. Djako, M. Gnamke, A. Kamognen, A. Kemajou, J.M. Koné, A. N'Diaté, A. Sako, M. Koita et D. Stamoukos, '*Efficacité Energétique de la Climatisation en Pays Tropical*', Tome 1- Conception des Nouveaux Bâtiments, IEPF, Chap. 1, une Méthode de Calcul Simplifié de Bilan Thermique de Climatisation, 35 p., 2003.

[5] O. Coulibaly, F. Kuznik, D. Baillis and A. Ouedraogo, '*Etude de l'influence des Matériaux de Construction sur les Consommations d'Energie en Climat Tropical Sec*', IBPSA France, Moret sur Loing 09 au 10 Novembre, 2010.

[6] Centre Scientifique Technique du bâtiment, CSTB, '*Réglementation Thermique, Règles TH-I, Caractérisation de l'Inertie Thermique*', 32 p., Novembre, 2000.

[7] Direction Générale de l'Energie, DGE, '*Audit Energétique et Stratégie Energétique Domestique*', SED, Ministère de l'Energie et des Mines, Burkina Faso, 2003.

[8] Institut de l'Energie et de l'Environnement de la Francophonie, IEPF, '*L'Architecture Bioclimatique*', 2008. http://www.iepf.org/ressources/ressources-pub.php?id=2&annee=2008

[9] S.A. Klein, W.A. Beckman; J.W. Mitchell, J.A. Duffie, N.A. Duffie, T.L. Freeman, J.C. Mitchell, J.E. Braun, B.L. Evans, J.P. Kummer, R.E. Urban, A. Fiksel, J.W. Thornton, N.J. Blair, P.M. Williams, D.E. Bradley, T.P. McDowell, M. Kummert and D.A. Arias, '*TRNSYS, Version 16, User Manual*', Solar Energy Laboratory, University of Wisconsin, 2006.

[10] F. Kreith and J.F. Kreider, '*Principles of Solar Engineering*', 778 p. 1978.

[11] J.J. Roux, '*Proposition de Modèles Simplifiés pour l'Etude du Comportement Thermique des Bâtiments*', Thèse de Doctorat, INSA de Lyon. 201 p. 1984.

[12] O. Sidler, '*L'Inertie Thermique en Climat Méditerranéen: Confort et Consommations d'Energie*', Colloque- Montpellier, 15 Mai 2003.

[13] M. Stathopoulou, C. Cartalis, and N. Chrysoulakis, '*Using Midday Surface Temperature to Estimate Cooling Degree-Days from NOAA-AVHRR Thermal Infrared Data: An Application for Athens, Greece*', Solar Energy In Urban Ventilation, Vol. 80, N°4, pp. 414 – 422, 2006.

[14] T. Catalina, J. Virgone, J.J. Roux et E. Blanco, '*Effet de l'Inertie Thermique, de la Surface Vitrée et du Coefficient de Forme sur les Besoins en Chauffage d'une Habitation*', International Building Performance Simulation Association, IBPSA France, 2008.

APPENDIXES

A. The seven stories 'NEWANGO' Building

Fig. A.1: Photo of the building 'Newango'

B. Surface temperature figures

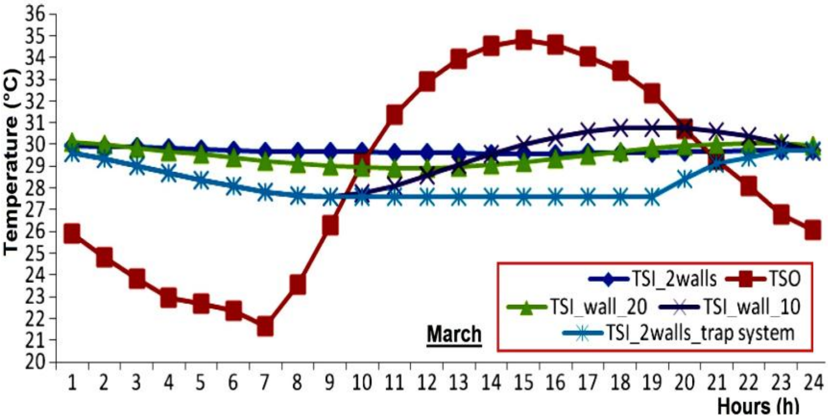

Fig. B.1: Time lag and heat absorption during March

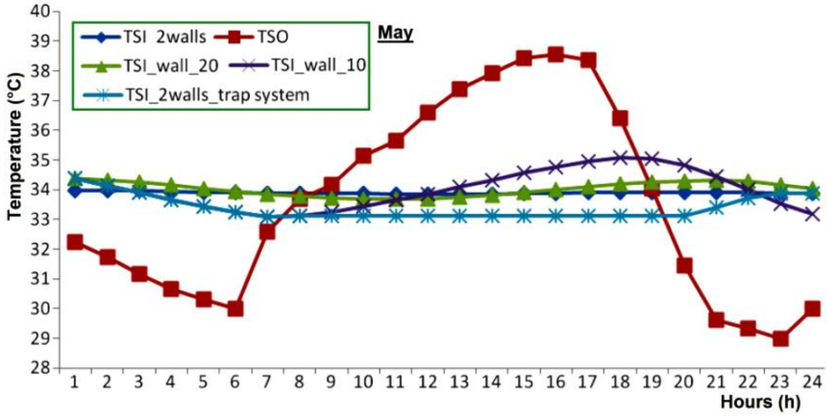

Fig. B.2: Time lag and heat absorption during May

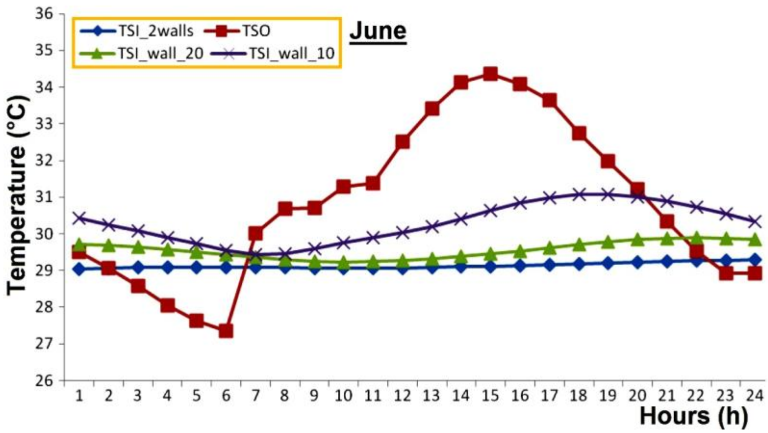

Fig. B. 3: Time lag and heat absorption during June

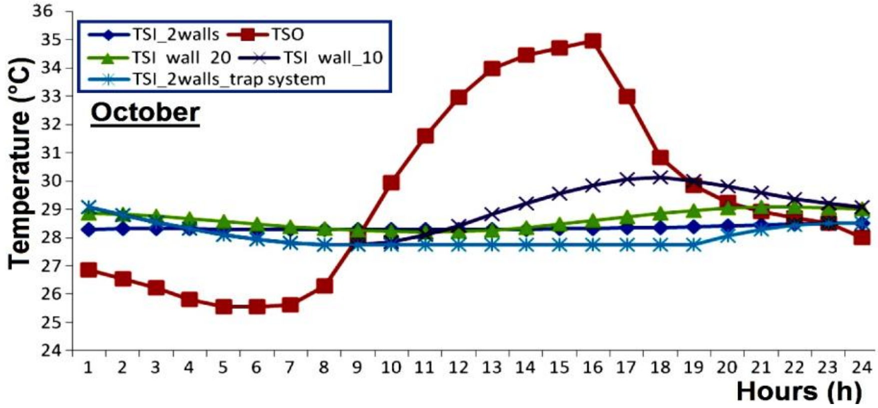

Figure B.4: Time lag and heat absorption during October